*Astronomy & Astrophysics* manuscript no. M31˙spitoni˙3
January 23, 2013




# The Effects of radial inflow of gas and galactic fountains on the chemical evolution of M31

E. Spitoni[1] ⋆, F. Matteucci[2], and M. M. Marcon-Uchida[3]

[1] Department of Mathematics, University of Évora, R. Romão Ramalho 59, 7000 Évora, Portugal
[2] I.N.A.F. Osservatorio Astronomico di Trieste, via G.B. Tiepolo 11, I-34131, Italy
[3] Núcleo de Astrofísica Teórica, Universidade Cruzeiro do Sul, Rua Galvão Bueno 868, Liberdade, 01506-000, São Paulo - SP, Brazil

Received xxxx / Accepted xxxx

**ABSTRACT**

*Context.* Galactic fountains and radial gas flows are very important ingredients in modeling the chemical evolution of galactic disks.
*Aims.* Our aim here is to study the effects of galactic fountains and radial gas flows in the chemical evolution of the disk of Andromeda (M31) galaxy.
*Methods.* We adopt a ballistic method to study the effects of galactic fountains on the chemical enrichment of the M31 disk. In particular, we study the effects of the landing coordinate of the fountains and the time delay in the pollution of the interstellar gas. To study the effects of radial flows we adopt a very detailed chemical evolution model. Our aim is to study the formation of abundance gradients along the M31 disk and also compare our results with the Milky Way.
*Results.* We find that the landing coordinate for the fountains in M31 is no more than 1 kpc from the starting point, thus producing negligible effect on the chemical evolution of the disk. We find that the delay time in the enrichment process due to fountains is no longer than 100 Myr and this timescale also produces negligible effects on the results. Then, we compute the chemical evolution of the M31 disk with radial gas flows produced by the infall of extragalactic material and fountains. We find that a moderate inside-out formation of the disk coupled with radial flows of variable speed can very well reproduce the observed gradient. We discuss also the effects of other parameters such a threshold in the gas density for star formation and an efficiency of star formation varying with the galactic radius.
*Conclusions.* We conclude that galactic fountains do not affect the chemical evolution of the M31 disk. The inclusion of radial gas flows together with an inside-out formation of the disk, produces a very good agreement with observations. On the other hand, if radial flows are not considered, one should assume a threshold in the star formation and a variable star formation efficiency, besides the inside-out formation to reproduce the data. We conclude that the most important physical processes in creating disk gradients are the inside-out formation and the radial gas flows. More data on abundance gradients both locally and at high redshift are necessary to confirm this conclusion.

**Key words.** ISM: jets and outflows - ISM: clouds - Galaxy: disk - Galaxy: open cluster and associations

## 1. Introduction

Galactic chemical evolution predicts how chemical elements are formed and distributed in galaxies. Galactic chemical evolution models follow the evolution of chemical abundances in the interstellar medium (ISM) is space and time. Chemical evolution is determined by the history of star formation, the stellar yields and gas flows. In particular, most of chemical evolution models deal with infall and outflow of gas in galaxies but very few models have taken into account the effects of radial flows and even less the effects of galactic fountains on the chemical evolution. Galactic fountains are created by supernova (SN) explosions in the disk of a galaxy: the gas ejected by multiple SN explosions occurring in OB associations reaches a certain height above the galactic plane and then, due to the potential well of the galaxy, it falls back onto disk. Bregman (1980) modeled first this process assuming that the gas falls back ballistically. Spitoni et al. (2008;2009) followed this approach and computed the effects of fountains on the chemical evolution of the Galactic disk and concluded that they are negligible; in fact, the gas ejected from the disk is likely to land very close to the place where it escaped. Moreover, the time delay with which the enriched supernova material is coming back into the ISM (∼ 100 Myr) does not influence substantially the chemical enrichment process. Gas infall is an important ingredient in the build -up of galactic disks and it produces radial gas flows, as shown first by Mayor & Vigroux (1981). In fact, the infalling gas has a lower angular momentum than the circular motions in the disk, and mixing with the gas in the disc induces a net radial inflow. Lacey & Fall (1985) computed a chemical model with radial flows and estimated that the gas inflow velocity is up to a few km $s^{-1}$. Later, Goetz & Köppen (1992) studied numerical and analytical models including radial flows. Chemical models with radial flows were studied more recently by Portinari and Chiosi (2000), Schönrich & Binney (2009) and Spitoni & Matteucci (2011), among others. In particular, Spitoni & Matteucci (2011) concluded that models assuming no inside-out formation of the Galactic disk need the presence of radial flows to explain the existence of abundance gradients. On the other hand, an inside-out formation of the disk coupled with a threshold in the star formation could equally reproduce the observed gradients although less steep than in the case of radial flows. Since the inside-out formation of disks seems to be observed at high redshift (Munoz-Mateos et al. 2007), the more reasonable conclusion was that both the inside-out process and radial flows should be at work in the Milky Way.

⋆ email to: spitoni@galaxy.lca.uevora.pt

Here, we plan to compute the chemical evolution of the disk of M31 including both the effects of galactic fountains and radial gas flows. We will start by adopting a model of chemical evolution of M31 developed by Marcon-Uchida et al. (2010) including inside-out formation of the disk but no fountains nor radial flows. The paper is organized as follows: in Section 2 we describe the model of Spitoni et al. (2008) used to compute the fountains in M31 and in Section 3 the results of this model are described. In Section 4 the Marcon-Uchida et al. (2010) model plus the implementation of radial flows in it are described. In section 5 the results for the abundance gradients in M31 are shown. In section 6 some conclusions are drawn.

## 2. The Galactic fountain model of Spitoni et al. (2008)

In order to study galactic fountains, Spitoni et al. (2008) followed the evolution of a superbubble driven by supernova explosions in the Galactic disk. They described the superbubble evolution using the Kompaneets (1960) approximation. Here we do not enter into the details of this model and we just recall that Kompaneets (1960) founds analytical expressions for the shape of the bubble during its expansion in an exponential atmosphere with density:

$$\rho(z) = \rho_0 exp(-z/H), \tag{1}$$

where $\rho_0$ and $H$ are the disk density and scale height, respectively.

In Spitoni et al. (2008) we showed that the total time necessary for the growth of instabilities and for the fragmentation of the superbubble in terms of $\rho_0$, $H$, and the luminosity of the system $L_0$ is:

$$t_{final} = 4.37 \times \left(\frac{\rho_0 H^5}{L_0}\right)^{1/3}. \tag{2}$$

Once the top of the supershell reaches the height above the galactic plane related to the time $t_{final}$ (see eq. 2), the thin shell can leave the stellar disk and move towards the extra-planar gas. Ballistic models describe the gas as an inhomogeneous collection of clouds, subject only to the gravitational potential of the Galaxy. The way we consider the galactic fountain for M31 is identical to the model described in Spitoni et al. (2008), therefore we address the reader to that paper for all the details.

### 2.1. The galactic potential and the OB associations of M31

The potential well of M31 is assumed to be the sum of three components as suggested by Howley et al. (2008): a dark matter halo, a bulge and a disk. The dark matter halo gravitational potential is assumed to follow the Navarro, Frenk and White (1996) profile:

$$\Phi_h(r) = -4\pi G \delta_c \rho_c r_h^2 \left(\frac{r_h}{r}\right) \ln\left[\frac{r + r_h}{r_h}\right] \tag{3}$$

where $\delta_c$ is a dimensionless density parameter, $\rho_c$ is today's critical density with Hubble constant $h = 0.71$ in units of 100 km/s/Mpc, and $r_h$ is the halo scale radius (Navarro et al. 1996). The bulge gravitational potential is given by (Hernquist 1990):

$$\Phi_b(r) = -\frac{GM_b}{a_0 + r} \tag{4}$$

where $a_0$ is the scale radius and $M_b$ is the bulge mass.

For the disk potential we have chosen the axisymmetrical Miyamoto & Nagai (1975) model which provides results that are comparable to those from the exponential disk used by Geehan et al. (2006). In cylindrical coordinates $(R, z)$ can be written as:

$$\Phi_d(R, z) = \frac{-GM_d}{\sqrt{R^2 + (R_d + \sqrt{z^2 + b^2})^2}}, \tag{5}$$

where Rd is the disk scale length and b is the vertical scale factor.

We use as done in Howley et al. (2008) the "Best-fit Model" values derived by Geehan et al. (2006) to describe the various parameters of M31, with the sole exception of $b$, the vertical scale factor, which was not a reported parameter. For $b$ we use the vertical scale height of the dust at a value of 0.1 kpc (Hatano et al. 1997). The values reported by Geehan et al. (2006) include the bulge mass, with $M_b = 3.3 \times 10^{10}$ M$_\odot$, the bulge scale factor, with $a_0 = r_b = 0.61$ kpc, the disk central surface density, with $\Sigma_0 = 4.6 \times 10^8$ M$_\odot$ kpc$^{-2}$, the disk scale radius, with $R_d = 5.4$ kpc, the halo scale radius, with $r_h = 8.18$ kpc.

For the interstellar medium (ISM) z-density profile we used eq. (1) where: $\rho_0 = n_0 \mu m_p$ is the density in the disk plane; $m_p$ is the proton mass and $\mu$ is mean molecular weight for the disk (assumed to be 0.61). At 8 kpc we fix $n_0 = 1$. In Banerjee & Jog (2008) it was shown that in the external regions of M31 the H values span the range between 300 and 400 pc. Then we tested at 8 kpc 2 scale heights : H= 200 pc, and H= 300 pc.

In our models we vary the number of SNeII in the OB association (SNe). We consider four possible OB associations containing 50, 100, 250, 500 SNe respectively. Assuming an explosion energy of $10^{51}$ erg, the luminosities $L_0$ of these OB associations are 5 $\times 10^{37}$, $10^{38}$, 2.5 $\times 10^{38}$ and 5 $\times 10^{38}$ erg s$^{-1}$ respectively. These numbers of massive stars in OB associations are consistent with observations of Magnier et al. (1994) who showed that the average number of massive stars in a OB association in M31 is $\simeq 250$.

## 3. The Results for the galactic fountains in M31

In this section we report the results concerning the fragmentation of the superbubble, the formation of the cloud and the study of the orbits of the galactic fountains in the cases of 8 kpc and 18 kpc. In Figs. 1 and 2 we report our results at 8 kpc for OB associations that can give rise to 250 SNeII, differing just in the height scale of the ISM: H=200 pc and H=300 pc respectively. In Fig. 3 is considered the case of 250 SNeII at 18 kpc with H=300. In Table 1 we report the ejection velocities for 50, 100, 250, and 500 SNeII at 8 kpc.

**Table 1.** The ejection velocities of our clouds as a function of the the number of SNeII and the height scale, in the case that the superbubble is fixed at 8 kpc.

| | $v_o$ [kms$^{-1}$] | $v_o$ [kms$^{-1}$] |
|---|---|---|
| SNe | H=200 | H=300 |
| 50 | 37 | 28 |
| 100 | 46 | 35 |
| 250 | 63 | 47 |
| 500 | 79 | 60 |

### 3.1. $R_0$ = 8 kpc, H=200 pc

We computed the model with a OB association composed by 250 SNeII, at 8 kpc, and ISM height scale is 200 pc. Using the Kompaneets approximation we obtain that the superbubble is already fragmented in clouds when its top side reaches $z_L$ = 636 pc ($\simeq$ 3H as found in Spitoni et al. 2008, Mac Low 1994). This phase lasts 11.7 Myr. In Fig. 1 we followed the orbit of our fountains. The initial velocity in this model is 63 km/s and our main result is that the clouds are generally thrown outward but the average landing coordinate is 8.29 kpc (only $\Delta$R=0.29 kpc). The average orbit time is 42.7 Myr.

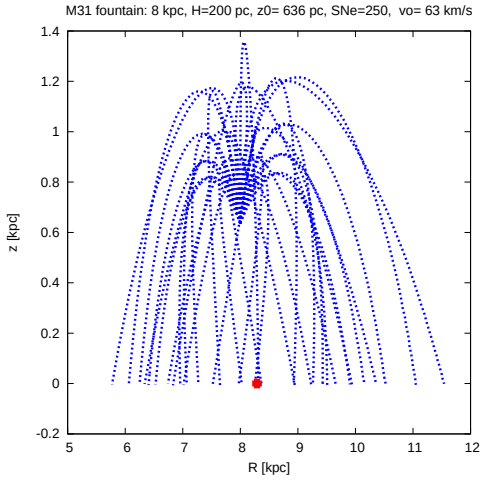


**Fig. 1.** Galactic fountains reported in the meridional plane with the spatial initial conditions: $(R, z)$=(8 kpc, 636 pc). The red filled circle on the $R$ axis is the average falling radial coordinate.

### 3.2. $R_0$ = 8 kpc, H=300 pc

Then we considered the model with the ISM medium height scale equal to 300 pc. The superbubble is already fragmented in clouds when its top side reaches $z_L$ = 955 pc ($\simeq$ 3H). This phase lasts 22.9 Myr. In Fig. 2 we followed the orbit of the fountains with an initial velocity of 47 km/s and our main result is that the clouds are generally thrown outward but the average landing coordinate is 8.15 kpc (only $\Delta$R=0.15 kpc). The average orbit time is 39.6 Myr.

### 3.3. $R_0$ = 18 kpc, H=300 pc

In Fig. 3 we followed the orbit of fountains with an initial velocity of 47 km/s and initial radial coordinate fixed at 18 kpc. Also in this case the clouds are generally thrown outward and the average landing coordinate is 18.89 kpc ($\Delta$R=0.89 kpc). The average orbit time is 147.1 Myr.

Because of the fact that the average landing coordinate differs for the throwing one for value always less than 1 kpc, we conclude that the effects of galactic fountains cannot affect directly the chemical evolution of M31, as we found for the Milky Way in Spitoni et al. (2008). Even if we consider the delay in the chemical evolution enrichment, due to the fact that the clouds originated in the galactic fountain processes take a finite time to orbit around the galaxy and fall back onto disk, we find that this effect is negligible, since the delays are the same as found

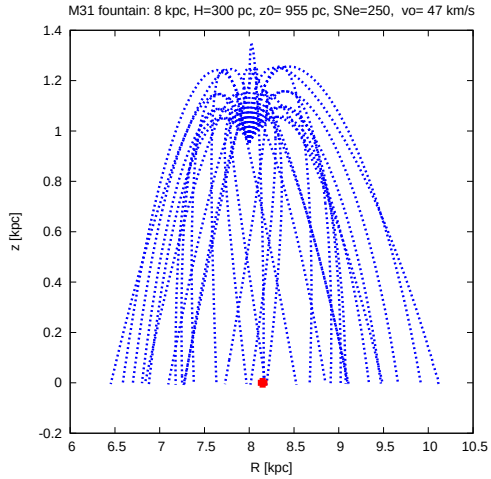


**Fig. 2.** Galactic fountains reported in the meridional plane with the spatial initial conditions: $(R, z)$=(8 kpc, 955 pc). The red filled circle on the $R$ axis is the average falling radial coordinate.

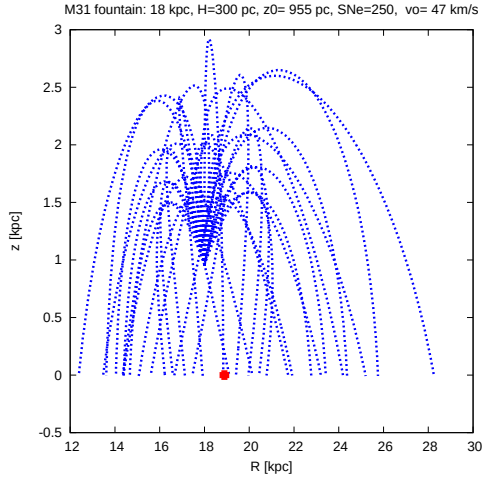


**Fig. 3.** Galactic fountains reported in the meridional plane with the spatial initial conditions: $(R, z)$=(18 kpc, 955 pc). The red filled circle on the $R$ axis is the average falling radial coordinate.

in Spitoni et al. (2010) for the Milky Way ($\sim$ 100 Myr). These delays have been proved not to have substantial effects on the process of chemical evolution.

However, the infalling gas onto the disk, originated by the galactic fountain, can be affected by the loss of angular momentum (Lacey & Fall 1985), in the same way as it happens for the primordial infall of gas. Therefore, this fountain gas can participate to the radial inflow of toward the galactic center, as we will show in the next Sections.

Concerning galactic fountains we also recall that in the MaGICC (Brooke & al. 2012a,b,c Pilkington & al. 2012b)) program, where hydrodynamical simulation in a cosmological context have been presented, fountains can be an important process during the galactic evolution.

First of all, in Brook et al. (2012a) it was shown that the majority of gas which loses angular momentum and falls into the central region of the galaxy during the merging epoch is blown back into the hot halo, with much of it returning later to form

stars in the disc. They proposed that this mechanism of redistribution of angular momentum via a galactic fountain, can solve the angular momentum/bulgeless disc problem of the cold dark matter paradigm. It was shown that this redistribution of angular momentum via large-scale galactic fountains can lead to the formation of massive disc galaxies which do not have classical bulges.

In the MaGICC program was also found that a extensive and significant mixing of fountain material throughout the disk can have an important impact on the disk's chemistry. In fact, Brook et al. (2012c) showed that disc stars are dominated by smoothly accreted gas; a not insignificant amount of gas that feeds the thin disc does come from gas-rich mergers. Much of this is recycled to the disc via the hot halo, after being ejected from the star forming regions of the galaxy during starbursts. This large scale galactic fountain process allows the recycled gas to gain angular momentum and aids in the suppression of the ubiquitous G-dwarf problem (Pilkington et al. 2012b).

The importance of strong feedback in securing correct scaling relations for disks and the correct coronal gas abundances in cosmological context has been discussed in Brook at al. (2012a, b, c) and Stinson et al. (2012). It was shown that the scale of outflows invoked in models matches the observed absorption line features of local galaxies (Prochaska et al. 2011; Tumlinson et al. 2011).

## 4. The chemical evolution model of M31

### 4.1. Our reference model for M31

In order to reproduce the chemical evolution of the M31 disk, we started from the one-infall chemical evolution model presented by Marcon-Uchida et al. (2010), where the details can be found and then we introduced radial flows in the same way as in Spitoni & Matteucci (2011) (see 4.1). In the starting model, the galactic disk is divided into several concentric rings which evolve independently without exchange of matter.

The disk is built up in an "inside-out" scenario which is a necessary condition to reproduce the radial abundance gradients when no radial gas flows are considered (Colavitti et al. 2008).

For the star formation rate (SFR) a Schmidt law was used:

$$\Psi(r,t) = \nu \Sigma^{k}_{gas}(r,t) \tag{6}$$

The star formation efficiency $\nu$ is assumed to vary with the galactocentric distance in such a way:

$$\nu = 24/R - 1.5\ Gyr^{-1} \tag{7}$$

until it reached a minimum value of 0.5 $\mathrm{Gyr}^{-1}$ and then is assumed to be constant.

This is suggested by the best model of Marcon-Uchida et al. (2010) in order to reproduce the present day gas profile of M31. This gas profile is different relative to that of the Milky Way: the gas increases with decreasing galactic radius and, after reaching a peak (at around 12 kpc) it decreases steeply towards the center, thus suggesting a different scenario. This trend is probably the signature of a very prominent spiral arm detectable in M31.

### 4.2. The chemical evolution models of M31 in the literature

Several studies in the past have been addressed to the modelling of the chemical evolution of M31, here we compare our reference model of Marcon-Uchida et al. (2010) model of M31 with some of them.

As done in Marcon-Uchida et al. (2010), the chemical evolution of M31 in comparison with that of the Milky Way has been discussed by Renda et al. (2005) and Yin et al. (2009). Renda et al. (2005) concluded that while the evolution of the Milky Way and M31 share similar properties, differences in the formation history of these two galaxies are required to explain the observations in detail. In particular, they found that the observed higher metallicity in the M31 halo can be explained by either a higher halo star formation efficiency, or a larger reservoir of infalling halo gas with a longer halo formation phase, which would lead to younger stellar populations in the M31 halo. Both pictures result in a more massive stellar halo in M31, which suggests a possible correlation between the halo metallicity and its stellar mass. Yin et al. (2009) concluded that M31 must have been more active in the past than the Milky Way although its current SFR is lower than in the Milky Way. They also concluded that the star formation efficiency in M31 must have been higher by a factor of two than in the Galaxy. However, by adopting the same SFR as in the Milky Way they failed in reproducing the observed radial profile of the star formation and of the gas, and suggested that possible dynamical interactions could explain these distributions. The main difference between the best model of M31 in Renda et al. (2005) and the model M31B of Marcon-Uchida et al. (2010), is the absence of any threshold in the star formation in the previous one.

In Yin et al. (2009) the infall prescription is the one presented by Boissier & Prantzos (2000), according to which the infall timescale is assumed to be correlated with the flat rotational velocity for the galaxy disk. In this work the star formation efficiency is proportional to $\Sigma_{gas}\Omega$, where $\Omega$ is the rotation speed of the gas, also in this model it was not consider a threshold in the star formation.

Carigi et a. (2012) presented a model of the chemical evolution of M31 computing also the Galactic Habitable Zones (GHZs) for this galaxy. We want to underline that they adopted the instantaneous recycling approximation, and therefore they can study only elements produced mainly by massive stars, such as oxygen.

### 4.3. The implementation of the radial inflow on M31 chemical evolution model

In Spitoni et al. (2011) we considered the case of radial inflow of gas for the Milky Way disk . Here we followed the same procedure to include radial gas flows in the disk of M31.

We define the $k$-th shell in terms of the galactocentric radius $r_k$, its inner and outer edge being labeled as $r_{k-\frac{1}{2}}$ and $r_{k+\frac{1}{2}}$. Through these edges, gas inflow occurs with velocity $\mathrm{v}_{k-\frac{1}{2}}$ and $\mathrm{v}_{k+\frac{1}{2}}$, respectively. The flow velocities are assumed to be positive outward and negative inward.

The radial flow term to be added into the chemical evolution equation is:

$$\left[\frac{d}{dt}G_i(r_k,t)\right]_{rf} = -\beta_k\, G_i(r_k,t) + \gamma_k\, G_i(r_{k+1},t), \tag{8}$$

where $\beta_k$ and $\gamma_k$ are, respectively:

$$\beta_k = -\frac{2}{r_k + \frac{r_{k-1}+r_{k+1}}{2}} \times \left[v_{k-\frac{1}{2}} \frac{r_{k-1}+r_k}{r_{k+1}-r_{k-1}}\right] \tag{9}$$

$$\gamma_k = -\frac{2}{r_k + \frac{r_{k-1}+r_{k+1}}{2}} \left[v_{k+\frac{1}{2}} \frac{r_k+r_{k+1}}{r_{k+1}-r_{k-1}}\right] \frac{\sigma_{A(k+1)}}{\sigma_{Ak}}, \tag{10}$$

where $\sigma_{A(k+1)}$ and $\sigma_{Ak}$ are the actual density profile at the radius $r_{k+1}$ and $r_k$, respectively.

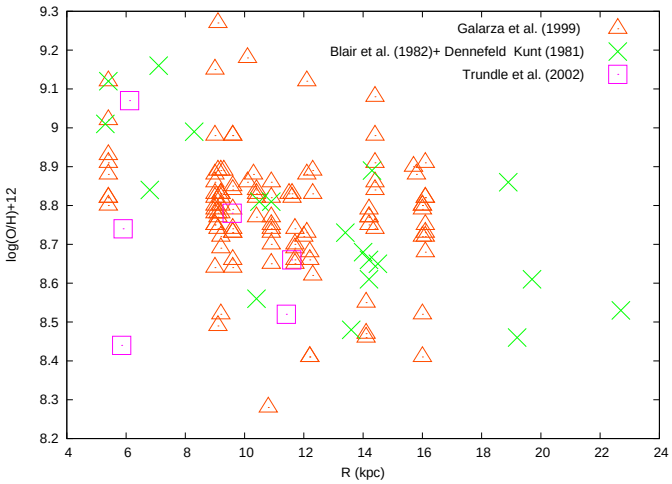


**Fig. 4.** Oxygen abundances observed in the HII Regions of M31. Data taken by: Galarza et al. (1999), Trundle et al. (2002), Blair et al. (1982) and Dennefeld & Kunth (1981).

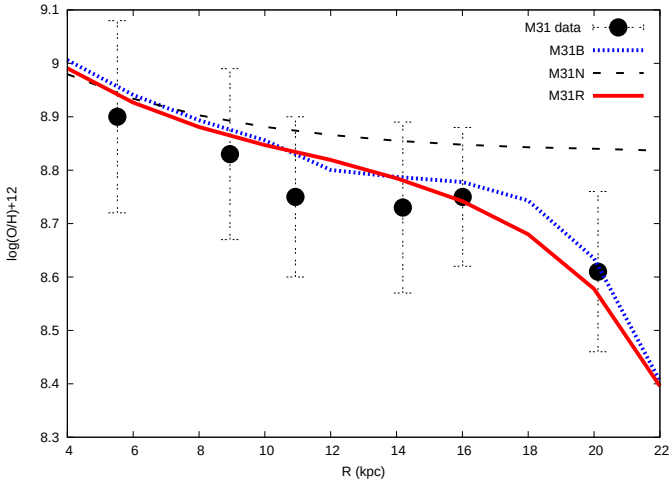


**Fig. 5.** Radial oxygen abundance gradient. The blue dotted line refers to the model M31B of Marcon-Uchida et al. (2010), the black dashed line to the M31N model with a constant SF efficiency, fixed at the value of 2 Gyr$^{-1}$, and without threshold, the red solid line refers to the best fit model M31R with radial inflow of gas. The filled circles and relatives error bars are the observed values from HII regions.

In our implementation of the radial inflow of gas in M31, only the gas that resides inside the Galactic disk within the radius of 22 kpc can move inward by radial inflow, as boundary condition we impose that there is not flow of gas from regions outside the ring centered at 22 kpc.

## 5. Radial flows Results

We have computed the oxygen gradient along the disk of M31 and compared to the available data. In particular, we adopted the same data as in Marcon-Uchida et al. (2010). In Fig. 4 we report the whole collection of the data that we used in this paper: Galarza et al. (1999) (HII regions), Trundle et al. (2002) (OB stars), Blair et al. (1982) and Dennefeld & Kunth (1981) (supernova remnants and HII regions).

To better understand the trend of the data, we divided the data into six bins as functions of the galactocentric distance. In each bin, we computed the mean value and the standard deviations for the studied element, as reported with black filled circles and relatives errors in Fig. 5. We are aware that there are some severe systematic uncertainties in each study that might justify larger error bars. In Fig. 5 we also plot the M31B model of Marcon-Uchida et al. (2010) without radial flows and we note that the model well fits the average trend of the data. In Table 2 we show the parameters of all the models we considered in this work: in particular, in column 2 there is the assumed inside-out law, in column 3 the assumed efficiency of star formation and in column 3 is indicated the presence or absence of radial flows. Model M31B is the best model adopted by Marcon-Uchida et al. (2010). This model contains an inside-out formation of the disk coupled with a variable efficiency of star formation and a threshold in the gas density, and it can reproduce the data without invoking radial flows. However, the existence of a threshold in the star formation process has been questioned by several GALEX studies (e.g. Boissier et al. 2007) and without such a threshold the model would not so well reproduce the external parts of the disk of M31. In addition, the hypothesis of a variable star formation efficiency is not proven and with a constant star formation efficiency the gradient would look much flatter. Therefore, we can conclude as in Spitoni & Matteucci (2011) did for the Milky Way disk, that radial gas flows can in principle be very important to reproduce the gradients along M31 disk, since all these processes are probably at work. To decide which of these processes is the most important in the formation of the disk, we will need more detailed data on the abundance, gas, and star formation rate gradients, as well as data on high redshift disks.

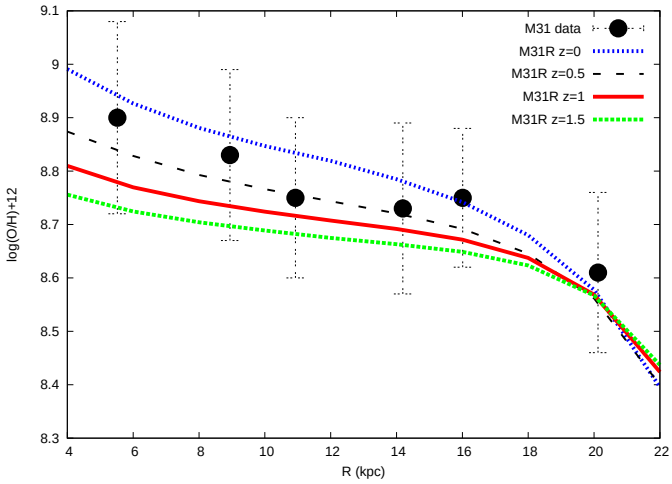


**Fig. 6.** Evolution of the radial oxygen abundance gradient for the model M31R (the best model in this study) as a function of the redshifts z=0, 0.5, 1, 1.5.

The first model we computed is M31N: this model has a constant star formation efficiency, fixed at the value of 2 Gyr$^{-1}$, it does not assume a star formation threshold no radial flows. The abundance gradient obtained with this model is shown with the

**Table 2.** Model parameters

| Models | $\tau_d$ | $\nu$ | Threshold | Radial inflow |
|---|---|---|---|---|
| M31B | 0.62 R (kpc) +1.62 Gyr | 24/R-1.5 $Gyr^{-1}$ | 5 $M_{\odot}pc^{-2}$ | no |
| M31N | 0.62 R (kpc) +1.62 Gyr | 2 $Gyr^{-1}$ | no | no |
| M31R | 0.62 R (kpc) +1.62 Gyr | 2 $Gyr^{-1}$ | no | yes, variable speed |

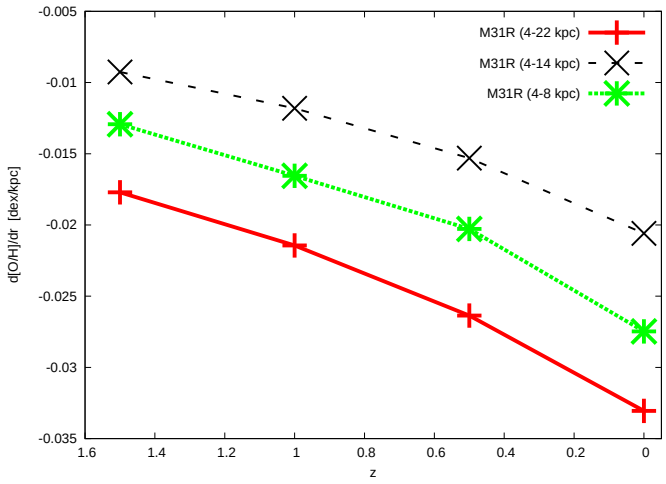


**Fig. 7.** Here we plot the oxygen abundance gradient, d[O/H]/dr, computed between 4-8 kpc, 4-14 kpc, and 4-22 kpc for the model M31R (best model), as function of redshift.

dashed line in Fig. 5. We see that this model fails to reproduce the gradient in the outer M31 regions.

Then we assumed the same parameters as in M31N but we included the radial flows with a variable velocity: in particular, we used a linear relation between the radial inflow velocity and galactocentric distance, as done in Spitoni & Matteucci (2011) for the disk of the Milky Way. In Fig. 5 we label with the red solid line this model, the M31R model. The radial inflow velocity pattern requested to reproduce the data follows this linear relation:

$$|v_r| = 0.05R + 0.45, \quad (11)$$

and spans the range of velocities between 1.55 and 0.65 km $s^{-1}$.

This model fits very well the O abundance gradient in the disk of M31, and we consider it our best model.

In Fig. 6 we report the abundance gradient evolution for oxygen as a function of the redshift for the our best model M31R. In Pilkington et al. (2012a) it was shown the time evolution of the metallicity gradients $dZ/dr$ [dex/ kpc] using a suite of disk galaxy hydrodynamical simulations and compared to the chemical evolution models of Chiappini et al. (2001) and Molla & Diaz (2005). We computed the gradient d[O/H]/dR for the model M31R, at redshifts z= 0, 0.5, 1, 1.5. In Fig. 7 we show the gradients for oxygen computed in the ranges 4-8 kpc, 4-14 kpc, and 4-22 kpc. We conclude that for the model M31R, where a variable gas inflow velocity is considered, a constant star formation efficiency, inside-out formation and no threshold in the star formation are assumed, the abundance gradient steepens with time, in accordance with the Chiappini et al. (2001) model.

The temporal evolution of the abundance gradients within cosmological hydrodynamical simulations has been shown to be sensitive to the spatial scale over which energy feedback operates (Pilkington et al 2012a). Conventional feedback schemes with ”localized” energy feedback result in steep gradients at high-redshift, which flatten with time towards redshift zero; conversely, conventional schemes which distribute energy more ”globally” and/or enhanced feedback schemes which drive significant outflows, circulation of the ISM, and radial gas flows, result in flat gradients at high-redshift, which evolve little with time. In this sense, the models presented here are entirely consistent with the latter enhanced feedback models (and vice versa).

## 6. Conclusions

In this paper we have studied the effects of galactic fountains and radial inflows of gas on the predictions of a detailed chemical evolution model for M31. Our main conclusions can be summarized as follows:

- Considering the average number of massive stars in a OB association in M31, the range of the cloud orbits is quite small. The clouds are generally directed outwards but the average landing coordinates differ from the throwing coordinates by values less than 1 kpc. Because of this fact, we conclude that galactic fountains cannot affect the chemical evolution of M31, as we found for the Milky Way in Spitoni et al. (2008). The reason for that is that inside 1 kpc, such as in the solar neighborhood, the gas is well mixed.
- The average time delay produced by a galactic fountain generated by an OB association in M31 is $\simeq$ 100 Myr. As we suggested for the Milky Way, in Spitoni et al. (2009), such a small delay time has a negligible effect on the abundance gradients in the Galactic disk.
- We started by adopting the best chemical evolution model of Marcon-Uchida et al. (2010) for the disk of M31. This model, in order to reproduce the observed abundance gradient, needs to assume a threshold in the star formation and an inside-out formation plus a star formation efficiency varying with the galactocentric distance. However, the existence of a threshold in the star formation has been questioned and the variable efficiency of star formation with galactocentric distance is not strongly physically motivated. On the other hand, a moderate inside-out formation for galactic disks seems to be observed at high redshift (Munoz-Mateos et al. 2007).
- The radial gas flow velocity, that we have found to be most consistent with the data, varies linearly with the galactocentric distance and spans a range between 0.65 and 1.55 km $s^{-1}$. This conclusion holds for the M31 chemical evolution

model with inside-out formation, without threshold, and a constant star formation efficiency fixed at 2 $Gyr^{-1}$.
- We showed that the abundance gradient d(O/H)/dr steepens with time for our best model which assumes no gas threshold in the star formation, an inside-out formation of the disk, a constant star formation efficiency along the disk and radial gas flows.
- Finally, we conclude, in agreement with Spitoni & Matteucci (2011), that also for M31 the radial gas flows can be very important to reproduce the gradients along the disk, although an inside-out formation coupled with a variable efficiency of star formation and threshold in gas density can also closely reproduce the data without radial flows. To decide which of these processes are the most relevant in the formation of the disk, we will need more detailed and precise data on the abundance, gas, and star formation rate gradients in M31, as well as more data on high redshift disks.

*Acknowledgements.* We thank the referee B. K. Gibson for his suggestions which improved the paper. E. Spitoni acknowledges financial support from the FCT by grant SFRH/BPD/78953/2011. F. Matteucci aknowledges financial support from PRIN MIUR 2010-2011, project "The Chemical and dynamical Evolution of the Milky Way and Local Group Galaxies", prot. 2010LY5N2T. M. M. Marcon-Uchida acknowledges financial support from FAPESP (2010/17142-4).

## References

Banerjee, A., & Jog, C. J., 2008, ApJ, 685, 254
Blair, W. P., Kirshner, R. P., Chevalier, R. A., 1982, ApJ, 254, 50
Boissier, S., Gil de Paz, A., Boselli, A., et al. 2007, ApJS, 173, 524
Boissier, S., Prantzos, N. 2000, MNRAS, 312, 398
Bregman, J. N. 1980, ApJ, 365, 544
Brook, C. B., Stinson, G., Gibson, B. K., Roskar, R., Wadsley, J., Quinn, T., 2012a, MNRAS, 419, 771
Brook, C. B., Stinson, G., Gibson, B. K., Roskar, R., Wadsley, J., Quinn, T., 2012b, MNRAS, 424, 1275
Brook, C. B., Stinson, G., Gibson, B. K., Kawata, D., House, E. L., Miranda, M. S.; Macci, A. V., et al., 2012c, MNRAS, 426, 690
Carigi, L., Meneses-Goytia, S., Garcia-Rojas, J., 2012, arXiv:1208.4198
Chiappini C., Matteucci F., Romano D., 2001, ApJ, 554, 1044
Colavitti, E., Matteucci, F., Murante, G. 2008, A&A, 483, 401
Dennefeld, M., & Kunth, D. 1981, AJ, 86, 989
Galarza, V. C., Walterbos, R. A. M., Braun, R. 1999, AJ, 118, 2775
Geehan, J. J., Fardal, M. A., Babul, A., Guhathakurta, P. 2006, MNRAS, 366, 996
Goetz, M., Koeppen, J., 1992, A&A, 262, 455
Kompaneets, A. S., 1960, Soviet Phys. Dokl., 5, 46
Hatano, K., Branch, D., Fisher, A., Starrfield, S. 1997, AJ, 487, L45
Hernquist, L. 1990, AJ, 356, 359
Howley, K. M., Geha, M., Guhathakurta, P., Montgomery, R. M.,Laughlin, G., Johnston, K. V., 2008, ApJ, 683, 722
Lacey C.G., & Fall M., 1985, ApJ, 290, 154
Magnier, E., Prins, S., Haiman, Z., Battinelli, P., van Paradijs, J., Lewin, W. H. G., van der Klis, M., Hasinger, G., Supper, R., Trumper, J., 1994, ESOC, 51, 904
Marcon-Uchida, M. M., Matteucci, F., Costa, R. D. D., 2010, A&A, 520, 35
Mayor M., Vigroux L., 1981, A&A 98, 1
Miyamoto, M., & Nagai, R. 1975, PASJ, 27, 533
Molla, M., Ferrini, F., Diaz, A. I., 1997, ApJ, 425, 519
Munoz-Mateos, J. C., Gil de Paz, A., Boissier, S., Zamorano, J., Jarrett, T., Gallego, J., Madore, B. F. 2007, ApJ, 658, 1006
Navarro, J. F., Frenk, C. S., White, S. D. M., 1996, ApJ, 462, 563
Pilkington, K., Few, C. G., Gibson, B. K., Calura, F., Michel-Dansac, L., Thacker, R. J., Molla, M., Matteucci, F., et al., 2012a, A&A, 540A, 56
Pilkington, K., Gibson, B. K., Brook, C. B., Calura, F., Stinson, G. S., Thacker, R. J.; Michel-Dansac, L., 2012b, MNRAS, 425, 969
Portinari, L., Chiosi, C., 2000, A&A, 355, 929
Prochaska J. X., Weiner B., Chen H.-W., Mulchaey J., Cooksey K., 2011, ApJ, 740, 91
Renda, A., Kawata, D., Fenner, Y., Gibson, B. K., 2005, MNRAS, 356,1071
Schönrich, R., & Binney, J, 2009, MNRAS, 396, 203
Spitoni, E., Recchi, S., Matteucci, F., 2008, A&A, 484, 743
Spitoni, E., Matteucci, F., Recchi, S., Cescutti, G., Pipino, A.,2009, A&A, 504, 87
Spitoni, E., Matteucci, F. ,2011, A&A, 531, 72
Stinson, G. S., Brook, C., Prochaska, J. X., Hennawi, J., Shen, S., Wadsley, J., Pontzen, A., at al., 2011, MNRAS, 425, 1270
Trundle, C., Dufton, P. L., Lennon, D. J., Smartt, S. J., Urbaneja, M. A. 2002, A&A, 395, 519
Tumlinson J., Thom C., Werk J. K., Prochaska J. X., Tripp T. M., Weinberg D. H., Peeples M. S., OMeara J. M., Oppenheimer B. D., et al., 2011, Science, 334, 948
Yin, J., Hou, J. L., Prantzos, N., Boissier, S., Chang, R. X., Shen, S. Y., Zhang, B., 2009, A&A, 505, 497